

Sediment Nitrogen Fixation: a Call for Re-evaluating Coastal N Budgets

Silvia E. Newell^{1,2} · Mark J. McCarthy^{2,3} · Wayne S. Gardner³ · Robinson W. Fulweiler^{1,4}

Received: 1 May 2015 / Revised: 28 April 2016 / Accepted: 20 May 2016 / Published online: 14 June 2016
© Coastal and Estuarine Research Federation 2016

Abstract Coastal ocean primary productivity is often limited by nitrogen (N) availability, which is determined by the balance between N sources (e.g., N-fixation, groundwater, river inputs, etc.) and sinks (e.g., denitrification, sediment burial, etc.). Historically, heterotrophic N-fixation in sediments was excluded as a significant source of N in estuarine budgets, based on low, indirectly measured rates (e.g., acetylene reduction assay) and because it was unnecessary to achieve mass balance. Many recent studies using net N₂ flux measurements have shown that sediment N-fixation can equal or exceed N₂ loss. In an effort to quantify N₂ production and consumption simultaneously, we measured N-fixation and denitrification directly in sediment cores from a temperate estuary (Waquoit Bay, MA). N-fixation, dissimilatory nitrate reduction to ammonium, and denitrification occurred simultaneously, and the net N₂ flux shifted from uptake (N-fixation) to efflux (denitrification) over the 120-h incubation. Evidence for N-fixation included net ²⁸N₂ and ³⁰N₂ uptake, ¹⁵NH₄⁺ production from ³⁰N₂ additions, ¹⁵N_{organic matter} production, and *nifH* expression. N-fixation from ³⁰N₂ was up to eight times higher than potential denitrification. However, N-fixation calculated

from ¹⁵NO₃⁻ was one half of the measured fixation from ³⁰N₂, indicating that ¹⁵NO₃-isotope labeling calculations may underestimate N-fixation. These results highlight the dynamic nature of sediment N cycling and suggest that quantifying individual processes allows a greater understanding of what net N₂ fluxes signify and how that balance varies over time.

Keywords Heterotrophic nitrogen fixation · Denitrification · DNRA · Coastal nitrogen budget

Introduction

The net nitrogen (N) inventory in marine ecosystems is determined by the balance between N losses (e.g., denitrification and burial) and new N production (e.g., N-fixation, atmospheric deposition, and riverine inputs). However, the N cycle is more dynamic and intricate than observed historically, as new pathways and organisms become incorporated into our understanding. In addition to the major pathways of the N cycle—N-fixation, organic matter remineralization, nitrification (oxidation of ammonium to nitrate), and denitrification (the stepwise reduction of nitrate to N₂ gas)—we now know that other processes play a key role in the marine environment. Additional nitrate reduction pathways—dissimilatory nitrate reduction to ammonium (DNRA; Koike and Hattori 1978) and N₂ production via anaerobic ammonium oxidation (anammox, Mulder et al. 1995)—play a more significant role in the environment than previously thought (Burgin and Hamilton 2007; Lam et al. 2009). Previously unknown microorganisms mediating N pathways, such as unicellular N-fixers (e.g., cyanobacteria, Zehr and Turner 2001; heterotrophic bacteria, Welsh 2000) and ammonia-oxidizing archaea (Francis et al. 2005), may be significant or even dominant in the ocean. These new developments increase the complexity of

Communicated by David Reide Corbett

✉ Silvia E. Newell
silvia.newell@wright.edu

¹ Department of Earth and Environment, Boston University, Boston, MA 02215, USA

² Department of Earth and Environmental Sciences, Wright State University, 3640 Colonel Glenn Highway, Dayton, OH 45435, USA

³ University of Texas Marine Science Institute, Port Aransas, TX 78373, USA

⁴ Department of Biology, Boston University, Boston, MA 02215, USA

measuring and modeling the N inventory. This complexity is compounded by anthropogenic N-loading ultimately from the Haber-Bosch process, which adds three times as much N globally as biological N-fixation (Galloway et al. 2013). Understanding, mitigating, and modeling the impacts of this N-loading requires quantification of these N transformation rates.

Over the last decade, new evidence has shown a wider occurrence of N-fixation and a more diverse community of N-fixers than previously thought. For example, *Trichodesmium*, a well-studied filamentous cyanobacterium, was considered one of the few significant sources of new N to marine environments (Capone et al. 1997). However, unicellular cyanobacteria can also contribute substantially to pelagic marine N-fixation (Zehr and Turner 2001). Additionally, rates of heterotrophic N-fixation in coastal sediments are higher than measured previously. In the past, acetylene reduction assays were the primary method for measuring heterotrophic N-fixation in sediments. Rates measured with this technique were low (8.1×10^{-3} to $13 \mu\text{mol N m}^{-2} \text{h}^{-1}$) and not important to balance N budgets, leading to the conclusion that sediment N-fixation was not a significant N source (see reviews by Capone and Carpenter 1982; Howarth et al. 1988; Seitzinger and Garber 1987). However, this method significantly alters the active microbial community (Fulweiler et al. 2015). Newer methods have the advantage of not using inhibitors and preserving the redox gradient at the sediment-water interface (e.g., stable isotopes and direct measurements of dissolved gasses in whole-core incubations). These methods generally yield higher rates of sediment N-fixation when it is detected. Recent studies indicate that N-fixation (reported as negative values, indicating sediment N_2 uptake) can be a significant N source in coastal sediments (-12 to $-250 \mu\text{mol N m}^{-2} \text{h}^{-1}$ reported in: Gardner et al. 2006; Fulweiler et al. 2007; Mortazavi et al. 2012; McCarthy et al. 2015), reservoirs (approx. $-200 \mu\text{mol N m}^{-2} \text{h}^{-1}$; Grantz et al. 2012), and tidal flats ($-402.7 \mu\text{mol N m}^{-2} \text{h}^{-1}$; Vieillard and Fulweiler 2012).

Why and how N-fixation occurs in sediments are not well understood. For cyanobacteria, the expression of the nitrogenase (*nif*) operon is repressed by ammonium (Lindell and Post 2001), which is often replete in sediment pore water (e.g., Froelich et al. 1979). However, heterotrophic diazotrophs can have a much higher ammonium threshold ($>1000 \mu\text{M}$) before nitrogenase inhibition occurs (Welsh 2000). Knapp (2012) compiled results from numerous studies in a variety of sediments and documented N-fixation at in situ concentrations of up to $30 \mu\text{M NO}_3^-$ and/or $200 \mu\text{M NH}_4^+$. Therefore, other factors (e.g., oxygen, organic carbon availability) may regulate microbial composition and heterotrophic N-fixation rates in sediments. Sediment core incubations from Laguna

Madre, TX, showed increased net N-fixation after glucose additions (An et al. 2001).

It is difficult to measure denitrification and N-fixation in sediments simultaneously, as denitrification produces and N-fixation consumes N_2 gas. The geochemical factors determining the balance between denitrification and N-fixation (and, therefore, the net N_2 flux) are not well understood. Denitrification is influenced by oxygen concentration, as well as carbon and nitrate availability (Cornwell et al. 1999; Ward et al. 2009). Field and mesocosm studies (Fulweiler et al. 2007, 2013; Eyre et al. 2013) in Narragansett Bay, RI suggest that both the quality and quantity of available organic carbon may control the balance between these processes. However, rates of these processes have not been measured separately and simultaneously, and heterotrophic N-fixation has not been proven to occur in sediments beyond the observation of N_2 uptake. This study addresses both of those issues in Waquoit Bay, MA, a typical temperate, eutrophic estuary that has been shown to exhibit both net denitrification and net N-fixation in sediments (Foster and Fulweiler 2014).

We studied Waquoit Bay to investigate the balance between three major sediment N cycling processes (N-fixation, denitrification, and DNRA). We hypothesized that (a) N_2 production (defined as denitrification, including any anammox) and consumption (defined as N-fixation) occur simultaneously in sediments and (b) changes in oxygen and dissolved inorganic N (DIN) concentrations determine the net N_2 flux. The objectives of the study were to: (1) measure N-fixation, potential denitrification, and potential DNRA directly in heterotrophic marine sediments; (2) determine the relative contributions of denitrification and N-fixation to the net N_2 flux; and (3) understand the mechanisms controlling N-fixation and loss processes and how they are reflected in the total N_2 signal.

Methods

Waquoit Bay is a small (3.34 km^2), shallow, temperate estuary on the south shore of Cape Cod, Massachusetts. The bay is adjacent to a dense residential area, and N-loading to the bay doubled from 1930–1980 (Bowen and Valiela 2001). The total annual N load is calculated as $26,781 \pm 9.6 \text{ kg N y}^{-1}$ (Valiela et al. 2000). The Metoxit Point (MP) site is located in the main basin ($41^\circ 34' 08.80'' \text{ N}$, $70^\circ 31' 05.13'' \text{ W}$) near the mouth of the Quashnet River, which carries more than a third of the total mean annual N load at $9879 \pm 11.0 \text{ kg N y}^{-1}$ (Valiela et al. 2000). Despite this high N load, Foster and Fulweiler (2014) reported an average net N-fixation at MP in 2011 of $-21 \pm 12 \mu\text{mol N m}^{-2} \text{h}^{-1}$. The MP site is shallow ($\sim 2 \text{ m}$) with flocculent, organic-rich sediments (C/N ratio 8.6 ± 0.2 , Foster and Fulweiler 2014). Thus, Waquoit Bay is an ideal model system to investigate the dynamics of N production and loss in coastal sediments.

Sediment cores were incubated over 5 days and samples were collected for dissolved gas and major nutrients. Sediment cores were collected in October 2012 with a HYPOX pole corer and check valve system designed to keep the sediment-water interface (SWI) and overlying water (OLW) intact (Gardner et al. 2009). Sediment cores (7.6 cm diameter) were incubated in a continuous-flow system as described previously (e.g., McCarthy et al. 2013). Briefly, cores and overlying water were capped with gas-tight plungers fitted with gas-tight PEEK inflow and outflow tubing at ~3 cm above the SWI (OLW volume ~136 mL). Unfiltered bottom water (collected from ~15 cm above the SWI in the field) in gas-tight 25 L Tedlar bags was pumped through the OLW at 1–2 mL min⁻¹ (OLW residence time ~97 min).

Isotope additions were performed, and the cores were pre-incubated overnight (~12 h) in an environmental chamber at in situ temperature (20 ± 2 °C) until sampling began the next morning. Three treatments were conducted in triplicate: (1) control (no isotope addition); (2) 5 μM ³⁰N₂ (99 %, Cambridge stable isotope laboratories) and (3) 4 μM ¹⁵NO₃⁻ (K¹⁵NO₃, 99 atom%, Cambridge Isotope Laboratories). Tracer addition concentrations were kept low to mimic in situ concentrations as closely as possible. However, nitrate concentrations were very low (<0.2 μM to undetectable in the OLW), so the tracer addition represents >95 % of the nitrate

pool, and the denitrification and DNRA rates are therefore considered “potential.” To make stock solutions, ³⁰N₂ gas was added to deionized water in a 1 L Tedlar bag and shaken gently on a shaker table overnight; 20 mL of stock solution was added to the site water in 25 L Tedlar bags, and final ³⁰N₂ concentration was determined by membrane inlet mass spectrometry (MIMS). Cores were incubated under continuous-flow conditions for 120 h after amendments. Initial sampling (time 0) was completed ~12 h after the tracer additions. Water samples were collected from the inflow reservoir and outflow ports at 0, 5, 12, 24, 48, 72, 96, and 120 h for dissolved gasses (^{28/29/30}N₂, argon, oxygen) and dissolved inorganic nutrients (ammonium, nitrate, nitrate + nitrite, ortho-phosphate) (Table 1).

Dissolved gas samples were collected in 12 mL Exetainers (Labco, UK). The samples were filled from the bottom and overflowed by at least one volume before preserving with 25 μL of saturated ZnCl₂. Dissolved gas samples and cores were inspected carefully for bubbles, because bubble formation can strip N₂ if samples are not collected and handled properly, causing the N₂/Ar ratio to decrease and appear as N-fixation (Eyre et al. 2002). Additionally, oxygen levels remained below saturation, and incubations were conducted in the dark. All nutrient samples were filtered immediately with a 0.2 μm nylon filter (GE Osmonics) and stored frozen.

Table 1 Geochemical fluxes for each timepoint for all treatments in μmol N m⁻² h⁻¹

Time (h)	Ammonium	Nitrite	Nitrate	Ortho-phosphate	Oxygen
Control					
0	493 ± 110	0.3 ± 0.3	N.D.	31 ± 12	-1170 ± 120
5	540 ± 51	0.5 ± 0.1	N.D.	34 ± 8	-997 ± 97
12	333 ± 28	0.00	N.D.	21 ± 3	-703 ± 64
24	434 ± 55	0.4 ± 0.2	N.D.	22 ± 2	-1530 ± 520
48	256 ± 8	0.00	N.D.	12 ± 1	-1320 ± 17
72	237 ± 0.2	2.2 ± 0.5	N.D.	8 ± 2	N.M.
96	219	0.00	N.D.	10	-1210
120	255	0.40	N.D.	12	-1250
¹⁵NO₃					
0	778 ± 258	0.8 ± 0.8	-65 ± 1.7	46 ± 19	-1000 ± 240
5	523 ± 43	0.7 ± 0.4	-51 ± 10	30 ± 3	-743 ± 25
12	345 ± 97	2.0 ± 0.6	10.5 ± 5.8	16 ± 5	-673 ± 120
24	346 ± 46	6.4 ± 1.4	-28 ± 4.2	16 ± 3	-924 ± 280
48	307 ± 44	2.4 ± 1.2	-21 ± 5.8	13 ± 0.3	-1420 ± 84
72	439 ± 155	6.1 ± 0.2	-2.0 ± 2.3	19 ± 11	-1430 ± 160
96	380	0.6	-64	17	-846
120	429	1.5	-63	22	-952
³⁰N₂					
0	337 ± 26	0.06 ± 0.06	1.6 ± 0.5	15 ± 1	-756 ± 7
5	366 ± 39	0.04 ± 0.04	N.D.	17 ± 2	-756 ± 85
12	349 ± 29	N.D.	N.D.	14 ± 2	-939 ± 110
24	328 ± 24	0.5 ± 0.3	N.D.	12 ± 1	-1580 ± 120
48	308 ± 22	N.D.	N.D.	10 ± 0.3	-1380 ± 94
72	241 ± 51	2.8 ± 0.8	N.D.	5 ± 4	-1310 ± 340
96	423	5.3	N.D.	13	-1500
120	277	1.1	0.2	8	-1620

Mean and standard error are reported for three replicate cores through 24 h, mean and range for two replicate cores from 24 through 72 h, and values for one core at 96 and 120 h. Negative values indicate sediment uptake

The Exetainer vials were stored under water at in situ temperature (± 2 °C) until analysis. At 0, 24, 72, and 120 h, water samples were also collected for $^{15}\text{NH}_4^+$ analysis using high-performance liquid chromatography (HPLC; Gardner et al. 1995), and one core from each treatment was sacrificed and subcored with duplicate, sterile 10 mL cutoff syringes for $^{15}\text{N}_{\text{organic}}$ and molecular analysis. At time 0, one core was sacrificed. Due to sacrificing cores, three cores were incubated through 24 h, but only two cores remained at 48 and 72 h and one at 96 and 120 h for each treatment. The subcores for $^{15}\text{N}_{\text{organic}}$ isotope measurements were sectioned into 1 cm depths down to 3 cm and dried overnight at 60 °C.

Dissolved gasses ($^{28}\text{N}_2$, $^{29}\text{N}_2$, $^{30}\text{N}_2$, O_2 , and argon (Ar)) were measured on a quadrupole MIMS (Kana et al. 1994) in the Fulweiler Lab at Boston University. The MIMS was tested to determine if low-oxygen conditions would result in production of NO^+ (mass 30; Eyre et al. 2002; Kana and Weiss 2004) by using serial 1 mL 20 mM sodium dithionite additions to room temperature water standards (Kana and Weiss 2004; Hartnett and Seitzinger 2003). No significant change in the $^{28}\text{N}_2/\text{Ar}$ was observed with decreasing O_2 , and no additional mass 30 molecules were produced allowing the samples to be processed on the MIMS without a furnace to remove oxygen. Samples were normalized to air-equilibrated deionized water standards (18 and 29 °C). Precision (coefficient of variation) is $<0.5\%$ for N_2 concentrations and $<0.05\%$ for N_2/Ar , and accuracy is $<1.5\%$ for N_2 concentrations and $<0.5\%$ for N_2/Ar for the MIMS (Kana et al. 1994). The MIMS system has similar sensitivities for the three N_2 gas species (An et al. 2001). The standard error for the $^{30}\text{N}_2$ signal of the standards was 0.017 %, and the detection limit (calculated as three standard deviations of the standard values above the baseline) was 0.0054 μM .

Potential denitrification rates were calculated from the sum of $^{28}\text{N}_2$, $^{29}\text{N}_2$, and $^{30}\text{N}_2$ production and any calculated N-fixation in $^{15}\text{NO}_3^-$ -amended cores using a total isotope technique (An et al. 2001). The An et al. (2001) calculations assume that ^{14}N and ^{15}N bind randomly when forming N_2 gas (i.e., that $^{28}\text{N}_2$, $^{29}\text{N}_2$, and $^{30}\text{N}_2$ would show binomial distribution). Assuming the proportion of $^{15}\text{NO}_3^-$ is p and $^{14}\text{NO}_3^-$ is $1-p$, the N_2 production rates are calculated for $^{28}\text{N}_2$ as $(1-p)^2$, for $^{29}\text{N}_2$ as $2p(1-p)$, and for $^{30}\text{N}_2$ as p^2 . The An et al. 2001 equations use the $^{28}\text{N}_2$ flux to predict the expected $^{29}\text{N}_2$ and $^{30}\text{N}_2$ values, and then compare the measured $^{29}\text{N}_2$ and $^{30}\text{N}_2$ values to the predicted values. Any differences are attributed to N-fixation, and the N-fixation rate is calculated. The potential denitrification rate is calculated from the sum of the total N_2 flux added to the predicted N-fixation rate.

Potential DNRA was calculated from $^{15}\text{NH}_4^+$ production in the $^{15}\text{NO}_3^-$ -amended cores (An and Gardner 2002). Note that this method may overestimate actual DNRA because $^{15}\text{NH}_4^+$ production represents a potential rate from increased substrate, but simultaneously may underestimate DNRA from coupled

nitrification/denitrification of in situ ^{14}N (Gardner and McCarthy 2009). N-fixation was calculated from $^{28}\text{N}_2$, $^{29}\text{N}_2$, and $^{30}\text{N}_2$ concentrations and fluxes in the $^{15}\text{NO}_3^-$ -amended cores (An et al. 2001) and from the sum of $^{28}\text{N}_2$, $^{29}\text{N}_2$, and $^{30}\text{N}_2$ uptake minus the $^{30}\text{N}_2$ uptake due to diffusion in the $^{30}\text{N}_2$ -amended cores. The $^{30}\text{N}_2$ diffusion flux (F) was calculated from Fick's Law (Hamersley and Howes 2005):

$$F = (-\Phi \times D_a \times \Delta C)/x$$

where Φ is the sediment porosity, D_a is the apparent diffusion coefficient, ΔC is the change in concentration of N_2 across the sediment, and x is the thickness of the sediment layer. The diffusion flux was calculated at each time point by estimating the diffusion depth (x) at time (t) (Crank 1975):

$$x = \sqrt{(D_a \times t)}$$

Sediment porosity (0.83 ± 0.01) for MP was reported by Foster and Fulweiler (2014, 2015), and the apparent diffusion coefficient (7.7 to $8.2 \times 10^{-6} \text{ cm}^{-2} \text{ s}^{-1}$) was reported by An and Joye (2001), using the Boudreau (1996) calculations, for estuarine sediments.

Ammonium released from mineralization was estimated from sediment oxygen demand (SOD; the difference between oxygen concentrations in the inflow and outflow normalized for flow rate and surface area), assuming approximately 1 mol O_2 is required to respire each mole of $\sim\text{CH}_2\text{O}$, and assuming a C/N ratio of $\sim 9:1$ (Foster and Fulweiler 2014). We acknowledge that this assumption may be an overestimate, as some oxygen may be used in sulfur (re)oxidation.

Dissolved inorganic nutrients were measured on a Seal Auto Analyzer 3 with segmented flow injection using standard colorimetric techniques (Solorzano 1969; Grasshoff et al. 1999).

$^{14}\text{NH}_4$ and $^{15}\text{NH}_4$ concentrations and isotope ratios were measured using HPLC in the Gardner Laboratory at the University of Texas Marine Science Institute (Gardner et al. 1995), and enriched values were $\sim 1000\%$ greater than natural abundance of $^{15}\text{NH}_4$.

Sediment $^{15}\text{N}_{\text{organic}}$ measurements were performed by the Boston University Stable Isotope Laboratory on a EuroVector Euro EA elemental analyzer (Owens 1988). The elemental analyzer detection limit was 0.2 μg (the samples were three orders of magnitude greater), precision was within 1.5 %, and the samples were up to 128 % enriched. Triplicate samples were analyzed from the top 3 cm of sediment. The flux of N_2 fixed as organic matter was estimated from the mass of $^{15}\text{N}_{\text{organic}}$ as:

$$\text{Flux} = \frac{^{15}\text{N}_{\text{organic}} \text{mass} \times (\text{sample mass}/\text{sediment density}) \times \text{SA}}{\text{time}}$$

where SA is the surface area of the core, and sample mass is

the total mass of the dried sediment analyzed by the elemental analyzer. The $^{15}\text{N}_{\text{organic}}$ production is an underestimate of total production, as only $\sim 1\%$ of $^{28}\text{N}_2$ pool was labeled.

Dissolved gas and nutrient fluxes were calculated from concentrations:

$$(\text{Outflow} - \text{inflow}) \times \text{flow rate} / \text{core surface area} = \text{flux}$$

Statistical Analyses were performed using Excel and JMP software. One-way analysis of variance (ANOVA) or group ANOVA tests were used to determine significant differences at a 95 % confidence level. p values are reported throughout the text.

RNA was extracted from three depths of sediment subcores (0–1 m, 1–2, 2–3 cm) to quantify functional genes for N-fixation (the nitrogenase (*nifH*)) and denitrification (the nitrite reductase (*nirS*)). Extractions were performed using the MoBio RNA PowerSoil Total RNA Isolation and RNA PowerSoil® DNA Elution Accessory Kits per the manufacturer's specifications. DNA free (New England Biolabs) removed DNA from RNA samples, and samples were tested for contaminant DNA via gel visualization and PCR. Complementary DNA (cDNA) was synthesized using the SuperScript III FirstStrand Synthesis kit (New England Biolabs), and cDNA from the three depths were combined and quantified using a NanoDrop ND-1000 spectrophotometer (NanoDrop Technologies). A 361-bp *nifH* fragment was amplified using the Poly et al. (2001) PolF (5'-TGC GAY CCS AAR GCB GAC TC-3') and PolR primers (5'-ATS GCC ATC ATY TCR CCG GA-3'). A 256-bp *nirS* fragment was amplified using primers NirS1F (5'-CCT AYT GGC CGC CRC ART-3') and NirS3R (5'-TTC CTB CAY GAC GGC GGC-3') (Braker et al. 1998). All quantitative polymerase chain reaction (qPCR) standards were made as described previously (Newell et al. 2011) by cloning and purification of the PCR product followed by serial dilution of the cleaned plasmid. For *nifH* quantification, each 20 μL reaction included 10 μL Quantitect SYBR Green (Qiagen), 0.5 μL of each primer (10 μM), 8.5 μL reverse transcription-PCR-grade water (Ambion), and 1 μL template cDNA (100 ng). For *nirS* quantification, each 20 μL reaction included 10 μL Quantitect SYBR Green (Qiagen), 0.2 μL of each primer (100 μM), 9.1 μL RT-PCR-grade water (Ambion), and 0.5 μL template cDNA (50 ng). Quantitative PCR was performed on an ABI 7900ht real-time qPCR machine. The *nifH* thermal profile consisted of 95 $^{\circ}\text{C}$ for 10 min, followed by 40 cycles of denaturation at 95 $^{\circ}\text{C}$ for 15 s, annealing at 60 $^{\circ}\text{C}$ for 30 s, and elongation at 72 $^{\circ}\text{C}$ for 30 s (Fan Lu 2013). The *nirS* thermal profile began with 15 min at 95 $^{\circ}\text{C}$, then 40 cycles of 94 $^{\circ}\text{C}$ for 15 s, 55 $^{\circ}\text{C}$ for 30 s, and 72 $^{\circ}\text{C}$ for 30 s. After amplification, a melting curve was obtained by

heating the products to 95 $^{\circ}\text{C}$, cooling them to 65 $^{\circ}\text{C}$, and then gradually heating them to 95 $^{\circ}\text{C}$ at a rate of 0.2 $^{\circ}\text{C s}^{-1}$. The specificity of the qPCR products was confirmed by melting curve analysis. Each assay was carried out within a single assay plate to permit direct comparison of copy numbers between environmental DNA samples. Each assay included triplicate, no template control (NTC) wells, triplicates for each of the five standards, and triplicate environmental samples. Automatic analysis settings were used to determine the threshold cycle (Ct) values. The efficiencies for each standard curve were within the acceptable range of 90–110 %, and R^2 values were above 0.99. The gene copy numbers were calculated according to:

Gene copy number =

$$(\text{ng} \times \text{number mol}^{-1}) / (\text{bp} \times \text{ng g}^{-1} \times \text{g mol}^{-1} \text{ of bp})$$

and then converted to gene copy number per gram of sediment.

Results

Control and $^{15}\text{NO}_3^-$ cores exhibited decreasing net $^{28}\text{N}_2$ uptake through 72 h and then switched to an increasing net $^{28}\text{N}_2$ efflux (Fig. 1). Significant $^{30}\text{N}_2$ production (greater than the control, one-way ANOVA, $p=0.014$, $n=6$) in the $^{15}\text{NO}_3^-$ cores began at 24 h, but a large, positive net $^{28}\text{N}_2$ flux was not seen until 120 h (Fig. 2). Calculated potential denitrification rates (An et al. 2001) were low ($<7 \mu\text{mol N m}^{-2} \text{ h}^{-1}$) until 120 h, when the rate peaked at 40.5 $\mu\text{mol N m}^{-2} \text{ h}^{-1}$ (Fig. 3). *nirS* expression remained constant in the $^{15}\text{NO}_3^-$ cores until between 72 and 120 h, when it increased by four orders of magnitude (Fig. 4). In the control cores, *nirS* expression decreased from 0 to 72 h, then increased by two orders of magnitude from 72 to 120 h.

Potential DNRA was calculated from production of $^{15}\text{NH}_4^+$ in the $^{15}\text{NO}_3^-$ cores. DNRA was observed as production and efflux of $^{15}\text{NH}_4^+$ from $^{15}\text{NO}_3^-$ at 24 h (average \pm SE, 5.7 \pm 4.8 $\mu\text{mol N m}^{-2} \text{ h}^{-1}$) but not at 72 or 120 h (Table 2). The ammonium efflux from sediments was greater in the $^{15}\text{NO}_3^-$ cores than the control cores at 0 and 120 h (but not 24 h) (Table 1).

The $^{30}\text{N}_2$ cores showed net $^{28}\text{N}_2$ and $^{30}\text{N}_2$ uptake over 120 h (Fig. 1). $^{30}\text{N}_2$ uptake could not be explained by diffusion from the OLW to the sediments alone. The diffusion estimates for $^{30}\text{N}_2$ uptake from Fick's law ranged were on average 25 % of observed $^{30}\text{N}_2$ uptake values (which ranged from -15.0 ± 2.3 to $-52.6 \pm 1.7 \mu\text{mol N m}^{-2} \text{ h}^{-1}$) over time for diffusion into the entire core. The ratio of $^{30}\text{N}_2/^{28}\text{N}_2$ uptake was lower than predicted by diffusion

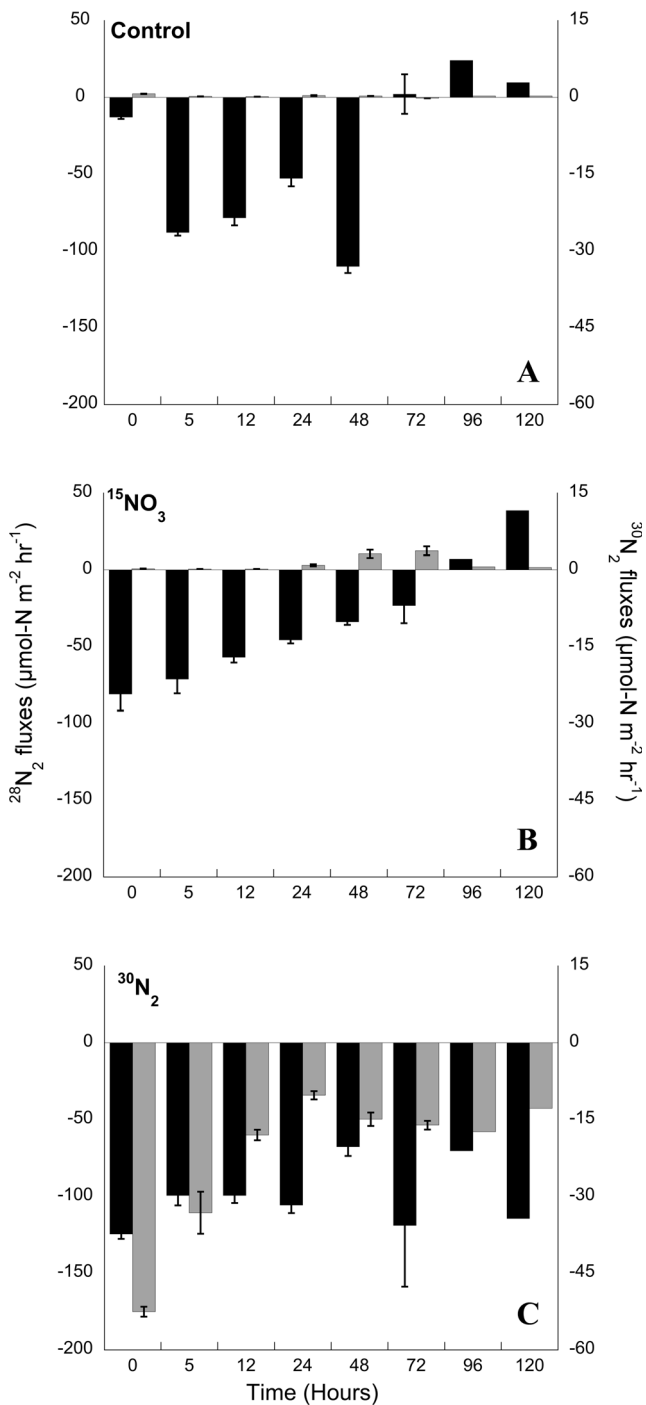


Fig. 1 Net N₂ fluxes in control (a), ¹⁵NO₃⁻ (b), and ³⁰N₂ cores (c). The ²⁸N₂ flux is shown in black (left y-axis) and the ³⁰N₂ flux is shown in gray (right y-axis). All fluxes are in μmol N m⁻² h⁻¹. Note the difference in the y-axis scales. Error bars depict the standard error

from their relative concentrations, but the net ²⁸N₂ flux is a balance between denitrification and N-fixation. ¹⁵NH₄⁺ effluxed from the sediments in the ³⁰N₂ cores through at least the first 24 h of sampling (Table 2) but was not detected after 72 h. ¹⁵N-biomass in the sediments from the ³⁰N₂ cores was detected at 72 and 120 h (0.83 ± 0.47 and

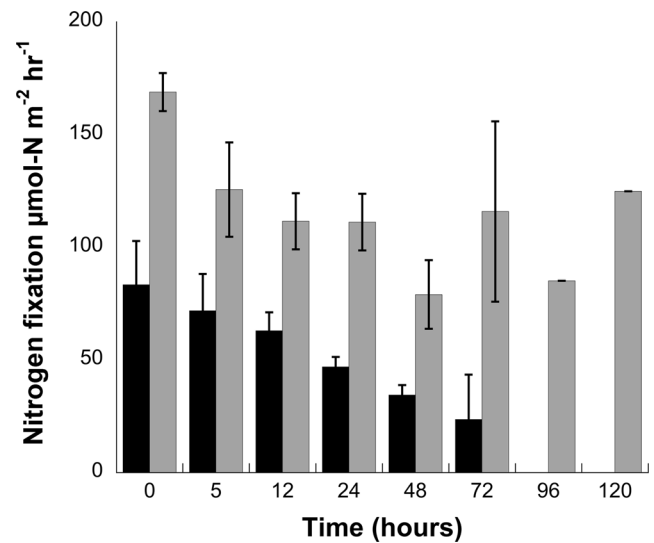


Fig. 2 N-fixation rates, as determined by directly observed fluxes (the sum of ²⁸N₂, ²⁹N₂, and ³⁰N₂ uptake minus the ³⁰N₂ uptake due to diffusion) from ³⁰N₂-amended cores (gray) and calculated from ²⁸N₂, ²⁹N₂, and ³⁰N₂ fluxes in ¹⁵NO₃⁻-amended cores using An et al. (2001) equations (black). Error bars depict the standard error

0.55 nmol N m⁻² h⁻¹, respectively). *nifH* functional gene expression was detected in all cores of all treatments over the course of the incubation and were maintained at a consistent level (Fig. 4).

N-fixation also was calculated from the sum of ²⁸N₂, ²⁹N₂, and ³⁰N₂ uptake in the ³⁰N₂ cores (Fig. 2), although ²⁹N₂ fluxes showed no discernible patterns in any treatment, and most rates were not significantly different from zero. ²⁸N₂ and ³⁰N₂ fluxes in the ³⁰N₂ cores were negative at every time point. ²⁸N₂ uptake was greatest at the initial sampling time (time “0” = -124 ± 3.1 μmol N m⁻² h⁻¹)

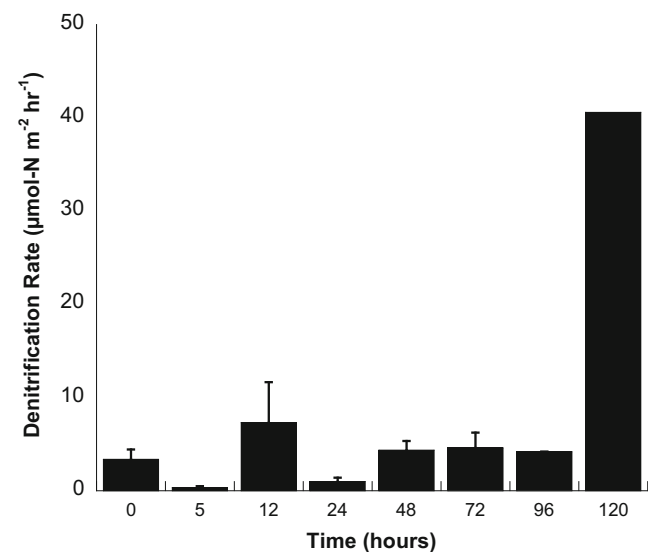


Fig. 3 Denitrification rates (as the sum of ²⁸N₂, ²⁹N₂, ³⁰N₂ production and calculated N-fixation, An et al. 2001) in the ¹⁵NO₃⁻ cores over time. Error bars depict the standard error

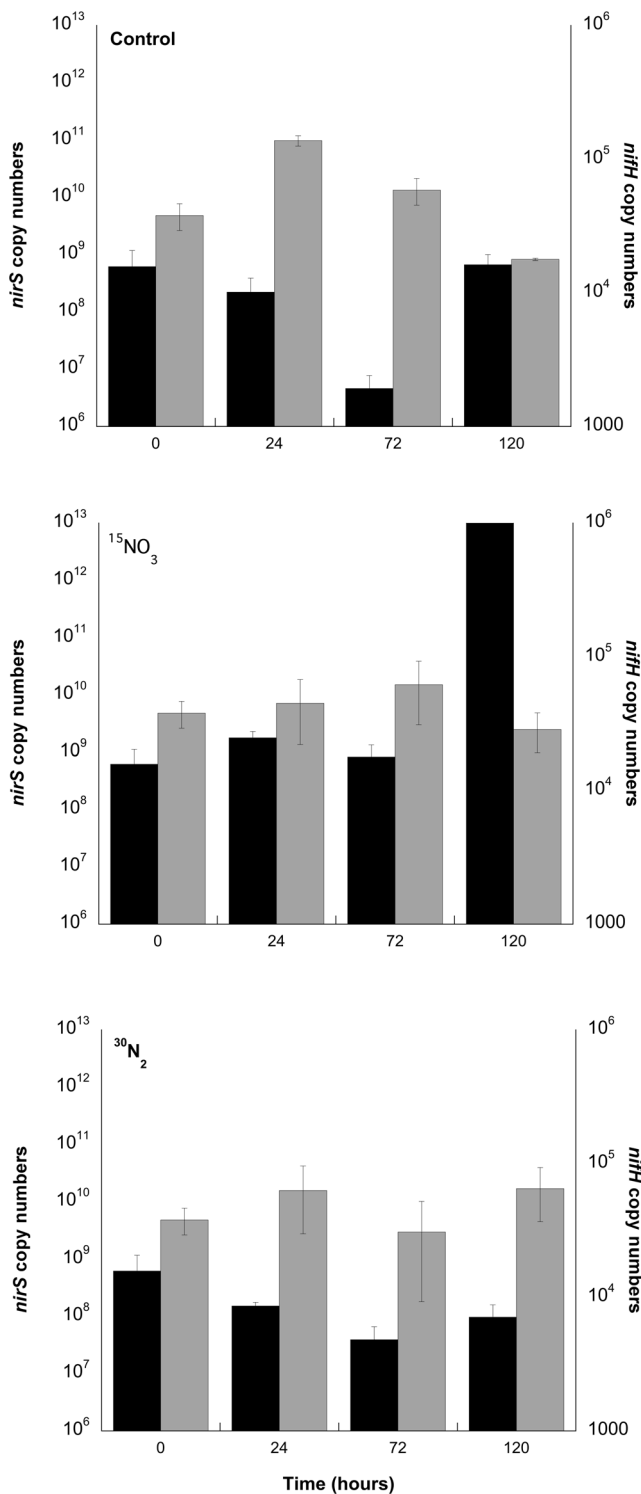


Fig. 4 Quantification of key functional gene transcripts for denitrification (*nirS*) and N-fixation (*nifH*) using RT-qPCR. Copies are per 100 ng template, *nirS* copies are shown in black, and *nifH* copies are shown in gray. Error bars depict the standard error

and then declined over the next 24 h. The $^{28}\text{N}_2$ fluxes had more uptake in the $^{30}\text{N}_2$ -amended cores than the control or $^{15}\text{NO}_3^-$ -amended cores (ANOVA, $p < 0.05$) during the first 48 h. N-fixation was also calculated from $^{28}\text{N}_2$, $^{29}\text{N}_2$,

Table 2 $^{15}\text{NH}_4^+$ flux ($\mu\text{mol N m}^{-2} \text{h}^{-1}$) mean and standard error at times 0 and 24 h

Time (h)	0	24
Treatment		
Control	0.4 ± 0.4	ND
$^{30}\text{N}_2$	0.6 ± 0.6	3.1 ± 3.0
$^{15}\text{NO}_3^-$	ND	5.7 ± 4.8

No $^{15}\text{NH}_4^+$ was detected in the overlying water at 72 or 120 h. $^{15}\text{NH}_4^+$ production in the $^{30}\text{N}_2$ cores is due to N-fixation of $^{30}\text{N}_2$, while production in the $^{15}\text{NO}_3^-$ cores is from DNRA

and $^{30}\text{N}_2$ concentrations and fluxes in the $^{15}\text{NO}_3^-$ cores according to An et al. (2001). The calculated rates declined over the first 72 h, but dropped to zero when the net N_2 signal was positive (Fig. 2).

Discussion

The control and $^{15}\text{NO}_3^-$ cores exhibited decreasing net $^{28}\text{N}_2$ uptake through 72 h and then switched to an increasing net $^{28}\text{N}_2$ efflux (Fig. 1), indicating that the system shifted from net N-fixation to net denitrification over the course of the 5-day incubation. This pattern may be explained in part by increased denitrification rates in response to nitrate inputs and oxygen decreases.

Nitrate Loss

DNRA was observed as production and efflux of $^{15}\text{NH}_4^+$ from $^{15}\text{NO}_3^-$ at 24 h (average \pm SE, $5.7 \pm 4.8 \mu\text{mol N m}^{-2} \text{h}^{-1}$), but not at 72 or 120 h (Table 2). Large $^{14}\text{NH}_4^+$ efflux from all treatments suggested that some fraction of the tightly recycled in situ nitrate may be reduced via DNRA as well. The NH_4^+ efflux from sediments was greater in the $^{15}\text{NO}_3^-$ cores than the control cores at 0 and 120 h (but not 24 h), but the differences were much greater than can be accounted for by $^{15}\text{NO}_3^-$ reduction alone. However, no $^{15}\text{NH}_4^+$ flux was observed after 24 h. Higher total $^{14}\text{NH}_4^+$ flux in $^{15}\text{NO}_3^-$ cores suggests that cation exchange mechanisms (Seitzinger et al. 1991; Gardner and St. John 1991) may be masking $^{15}\text{NH}_4^+$ release from sediments (as $^{15}\text{NH}_4^+$ replaces $^{14}\text{NH}_4^+$ between clay sheets). Regardless, DNRA is likely underestimated here, as the only definitive measurement is production of $^{15}\text{NH}_4^+$, and the relative fraction of $^{14}\text{NH}_4^+$ flux from DNRA is unknown.

Denitrification was calculated using a total isotope approach (An et al. 2001), as the sum of $^{28}\text{N}_2$, $^{29}\text{N}_2$, and $^{30}\text{N}_2$ production and calculated N-fixation. Calculated potential denitrification rates (An et al. 2001) peaked at $40.5 \mu\text{mol N m}^{-2} \text{h}^{-1}$ (Fig. 3), coinciding with the four orders of

magnitude increase in *nirS* transcript abundance at 120 h (Fig. 4). Similarly, in the control cores, *nirS* transcript abundance increased by two orders of magnitude from 72 to 120 h, coinciding with the shift from net N₂ uptake to efflux. There was a positive, linear correlation between the *nirS* transcript abundance and the potential denitrification rates ($R^2=0.99$, $p=0.003$, 98 % confidence). Thus, denitrification increased rapidly over the last 48 h of the incubation. The peak potential rate of 40.5 $\mu\text{mol N m}^{-2} \text{h}^{-1}$ falls within the denitrification rates previously measured for this system at other sites (October 1992, $190 \pm 59 \mu\text{mol N m}^{-2} \text{h}^{-1}$; October 1993, $38 \pm 0.5 \mu\text{mol N m}^{-2} \text{h}^{-1}$) reported by LaMontagne et al. (2002) using a different analytical method of measuring the N₂ flux (a gas chromatograph connected to a modified gas stripping device). Both denitrification and N-fixation rates are similar to the N₂ flux range measured in 2011 from nine cores at MP (-50.5 to $38.5 \mu\text{mol N m}^{-2} \text{h}^{-1}$, Foster and Fulweiler 2014).

From 0 to 24 h, sediment nitrate uptake was nearly balanced by DNRA and denitrification. However, at 120 h, potential denitrification was 33 % lower than the measured nitrate uptake (Fig. 6), and no DNRA was observed in the ¹⁵NO₃⁻ cores. These results suggest that the potential denitrification rates may be 1.5× higher than the total isotope calculations estimate. We hypothesize that this difference is due to these calculations (An et al. 2001) underestimating the co-occurring N-fixation, as the denitrification rate is ultimately calculated by adding the N-fixation rate to the total N₂ flux; therefore, if N-fixation is underestimated, so is denitrification.

Recent work in estuaries in Massachusetts (Koop-Jakobsen and Giblin 2010), Texas (Gardner et al. 2006) and Florida (Gardner and McCarthy 2009) showed that DNRA and denitrification can co-occur at similar rates. Additionally, a review by Giblin et al. (2013) reported that DNRA accounted for more than 30 % of the nitrate reduction at 26 of 55 coastal sites. The balance between these processes is not well understood, although DNRA and SOD were positively correlated, and denitrification was inversely correlated with both processes, in Florida Bay (Gardner and McCarthy 2009). An earlier study in Baffin Bay, TX (An and Gardner 2002) showed much higher rates of DNRA than denitrification, possibly due to the high sulfide concentrations in the sediments (which may inhibit denitrification, but enhance DNRA; Brunet and Garcia-Gil 1996).

Nitrate is tightly recycled in this system, as the in situ nitrate concentration in this study remained very low (<0.2 μM) or not detectable (Table 1). We observed DNRA in the first 24 h, but very low denitrification rates. Waquoit Bay also has very high organic carbon (620 μM dissolved organic carbon in Childs River groundwater, Hopkinson et al. 1998), supporting Tiedje's (1988) hypothesis that DNRA is more important in high-carbon, low-nitrate systems (Burgin and Hamilton 2007). While *nirS* expression shows denitrifying bacteria were present and actively expressing

the nitrite reductase gene throughout the incubation, these facultative anaerobes use oxygen preferentially when it is plentiful. DNRA was not observed after 24 h (although it may have been masked), while ³⁰N₂ production from denitrification increased. There was a strong correlation between ³⁰N₂ production in the ¹⁵NO₃⁻ cores and oxygen decline ($R^2=0.69$, $p<0.0001$, 98 % confidence). While no nitrate was added to the control cores, we observed a similar ~40 μM decrease in OLW oxygen concentration during the incubation (Fig. 5). As oxygen declined, both the control and the ¹⁵NO₃⁻ cores shifted to net denitrification (N₂ efflux) by 96 h (oxygen in the ³⁰N₂ cores was generally greater than but not significantly different from the control cores through the first 48 h, Fig. 5). Denitrifiers may compete more effectively with DNRA for nitrate when low-oxygen favors nitrate respiration (Körner and Zumft 1989).

Anammox typically accounts for <6 % of the total N₂ loss from shallow (<20 m) systems (Dalsgaard et al. 2005). Our results suggest that anammox was not a significant pathway in this study, as no ²⁹N₂ (e.g., significantly different from the control cores, $p=0.61$, ANOVA) was produced in the ¹⁵NO₃⁻ cores, even though >1 μM ambient NH₄⁺ was available. Likewise, anammox contributed ≤4 % of the total N₂ production in nearby Narragansett Bay, RI (Brin et al. 2014). However, while anammox bacteria are capable of reducing nitrate to nitrite reduction (Kartal et al. 2007), they ultimately can provide only ~10 % of the NO₂⁻ needed to oxidize ammonium.

N-fixation

Sediment N-fixation occurred throughout the experiment in the ³⁰N₂-amended cores. Multiple lines of direct evidence support this conclusion: (1) ¹⁵NH₄⁺ effluxed from the sediments in the ³⁰N₂ cores within at least the first 24 h of sampling (Table 2), (2) the ³⁰N₂ cores showed net ²⁸N₂ and ³⁰N₂ uptake (greater than diffusion) within 120 h (Fig. 1), (3) ¹⁵N-organic matter in the sediments from the ³⁰N₂ cores was detected at 72 and 120 h, and (4) *nifH* functional gene expression was detected in all cores of all treatments over the course of the incubation, indicating that N-fixers were both present and expressing nitrogenase genes (Fig. 4). N-fixation occurred at similar rates at the same station in Waquoit Bay in 2011 (Foster and Fulweiler 2014). The *nifH*-containing community was characterized by Newell et al. (2011) and dominated by δ -proteobacteria. N-fixation was determined from the sum of ²⁸N₂, ²⁹N₂, and ³⁰N₂ uptake minus the ³⁰N₂ uptake due to diffusion (~25 %) in the ³⁰N₂ cores (Fig. 2) and also calculated from ²⁸N₂, ²⁹N₂, and ³⁰N₂ concentrations and fluxes in the ¹⁵NO₃ cores (after An et al. 2001). We assume that N₂ uptake is attributed to sediment N-fixation and diffusion. However, although there are no reported values of N-fixation in the Waquoit Bay water column, work by

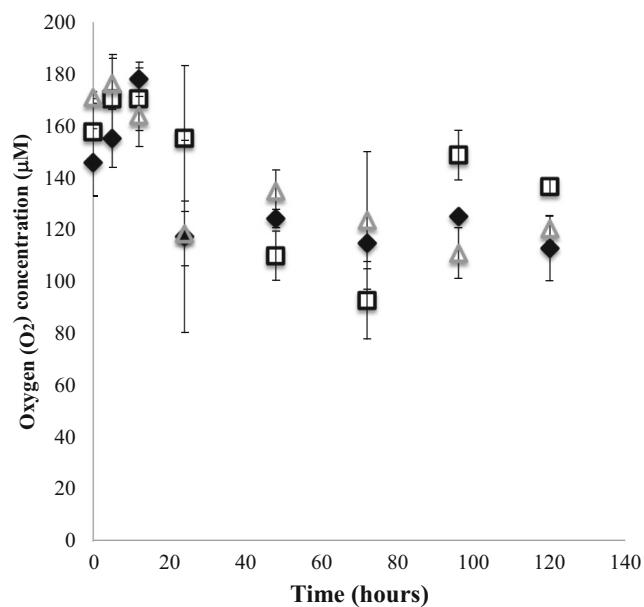


Fig. 5 Oxygen (O₂) concentrations (µM) from the outflow lines throughout the incubation. Oxygen in the control cores is shown as *black, filled diamonds*, in ¹⁵NO₃⁻-amended cores as *black, open squares*, and in ³⁰N₂-amended cores as *gray triangles*. Oxygen concentrations in the inflow did not decrease below 90 % of saturation. Error bars depict the standard error

Bentzon-Tilia et al. (2015) has highlighted the potential importance of simultaneous N-fixation by photoheterotrophic and heterotrophic bacteria and cyanobacteria in estuarine water columns. Although the cores were incubated in the dark and the OLW remained aerobic, we cannot rule out the possibility that some of the N₂ uptake could be attributed to water column N-fixation.

The ³⁰N₂ uptake rates were adjusted to account for diffusion within the core. This estimate may be a conservative estimate if meiofauna bioturbation speeds up diffusion. However, even in the extreme scenario that diffusion accounted for 100 % of the ³⁰N₂ uptake (which is unlikely due to the observation of ¹⁵N-organic matter and ¹⁵NH₄⁺ production), the ²⁸N₂ flux in those cores accounted for 80 % of the measured N-fixation rate. These calculated rates followed the same pattern initially as the direct rates: N-fixation was greatest at the initial sampling time (time “0” h, $-83.4 \pm 19.1 \mu\text{mol N m}^{-2} \text{h}^{-1}$) and then decreased, but the calculated rates were not detected by 96 h (Fig. 2). The N-fixation rates measured directly from the ³⁰N₂-amended cores were significantly (group ANOVA, $p=0.00012$, and paired t tests, $p<0.0001$) different from and approximately double the An et al. 2001 calculated rates from the ¹⁵NO₃⁻ cores. The calculated rates dropped to zero when the net N₂ signal was positive, despite their design to estimate simultaneous N-fixation and denitrification.

In situ dissolved inorganic N concentrations in the OLW were not high enough to inhibit N-fixation. Heterotrophic N-fixers, such as sulfate-reducing bacteria, can have a much higher threshold of ammonium concentrations required to (indirectly) repress expression of the *nif* operon than

cyanobacteria (Knapp 2012). Indeed, sulfur and sulfate reducers have been linked to sediment N-fixation in Narragansett Bay (Brown and Jenkins 2014; Fulweiler et al. 2013). In marine environments, N-fixation continued to occur in the presence of up to 30 µM NO₃⁻ and/or 200 µM NH₄⁺ (Knapp 2012). Millimolar concentrations of ammonium are required to shut off N-fixation by sulfate reducers (Welsh 2000), and 100 µM ammonium only slightly impairs N-fixation in *Pseudomonas stutzeri* A1015 (Desnoues et al. 2003). Pore water ammonium was not measured in this study, but the OLW concentration never exceeded 10 µM; thus, we believe that N-fixation was not inhibited by DIN concentrations in these incubations.

Despite the presence of ammonium, sediment conditions may favor N-fixation. Low-oxygen conditions are conducive to the obligatory anaerobic N-fixation pathway, and each N₂ fixed requires 8H⁺ and 8e⁻, and sediments have a high redox potential. In fact, enhanced shuttling of protons and electrons through the nitrogenase may be a response to strongly reducing conditions in sediments.

Coastal Nitrogen Budget

Coastal ecosystems inherently vary over time and space. Physical and geochemical conditions fluctuate daily with light and tides, as salt water exchanges with freshwater, and seasonally with temperature and river input (among other factors). The results presented here and in other studies (Table 3) indicate that sediment N₂ fluxes respond to changing conditions dynamically as the balance of denitrification and N-fixation is influenced by the supply of labile organic carbon, nitrate, oxygen, etc. (Burgin and Hamilton 2007). N₂ fluxes also vary on daily and yearly timescales. For example, the N dynamics in our core system shifted from net N-fixation to net denitrification over the course of the 120-h incubation. This may be in response to changing O₂ concentrations in the OLW (Fig. 5), which mimics the diel change in in situ oxygen, which declines (sometimes into hypoxia) at night in the summer. In Narragansett Bay, RI, interannual shifts occurred in net sediment N₂ flux, oscillating between average net denitrification and net N-fixation (Fulweiler and Heiss 2014). In Weeks Bay, Alabama, a year-long study showed a sinusoidal net N₂ flux, with N-fixation or denitrification as the dominant process varying on a monthly scale (Mortazavi et al. 2012). Individual sampling efforts produce snapshots, but longer-term sampling efforts across all seasons are required to determine how net N₂ fluxes fluctuate temporally.

Many recent studies indicate that N-fixation rates in coastal sediments can equal or exceed N₂ loss rates at times. Using whole-core incubations and direct measurements of dissolved gasses, sediment N-fixation rates similar to or exceeding denitrification have been reported in temperate and tropical estuaries, wetlands, and near-shore marine ecosystems (see

Table 3 Comparison of sediment core incubation studies reporting both N-fixation (N_2 uptake) and denitrification (N_2 production)

N-fixation ($\mu\text{mol N m}^{-2} \text{h}^{-1}$)	Denitrification ($\mu\text{mol N m}^{-2} \text{h}^{-1}$)	Method	Location	Study
0–97	0–90	MIMS $N_2/\text{Ar } ^{15}\text{NO}_3^-$ addition	Texas estuaries	Gardner and McCarthy (2006)
0–650 \pm 200	0–530	MIMS N_2/Ar	Narragansett Bay, RI	Fulweiler et al. (2007)
0–426 \pm 35	54 \pm 13–615 \pm 229	MIMS $N_2/\text{Ar } ^{15}\text{NO}_3^-$ addition	Lake Waco Wetland	Scott et al. (2008)
73 (1 observation)	76 \pm 22	MIMS N_2/Ar	Offshore Rhode Island	Heiss et al. (2012)
8–125	5–72	MIMS N_2/Ar acetylene inhibition (denitrification)	Weeks Bay, Alabama	Mortazavi et al. (2012)
4.0 (\pm 25.8)–28.1 (\pm 11.6)	9.1 (\pm 9.1)–63.6 (\pm 63.6)	MIMS N_2/Ar	Waquoit Bay, MA	Foster and Fulweiler (2014)
0–147 \pm 39	18 \pm 0.5–562 \pm 70	MIMS $N_2/\text{Ar } ^{15}\text{NO}_3^-$ addition	Gulf of Mexico hypoxic zone	McCarthy et al. (2015)
40–67	6.5–26.5 (seasonal averages)	MIMS N_2/Ar	Moreton Bay, Australia	Ferguson and Eyre (2013)
49 \pm 8–103 \pm 4	0–28 \pm 14	MIMS $N_2/\text{Ar } ^{15}\text{NO}_3^-$ and $^{30}\text{N}_2$ additions	Waquoit Bay, MA	This study

Error values are as reported by the authors in the original manuscript

Table 3), although denitrification rates may be higher averaged over time. Likewise, N-fixation and denitrification co-occurred within the same order of magnitude in our experiments. This co-occurrence of N-fixation and denitrification was supported by simultaneous measurement of *nifH* and *nirS* expression, and the control and $^{15}\text{NO}_3^-$ cores showed an increase in *nirS* corresponding with the shift in N_2 influx to efflux ($^{15}\text{NO}_3^-$, $R^2 = 0.99$, $p = 0.003$, 98 % confidence). These results are similar to those reported in a large mesocosm using Narragansett Bay sediments where both *nifH* and *nirS* expression were detected concurrently despite overall net denitrification rate measurements (Fulweiler et al. 2013).

Balancing the N budget in aquatic systems is desirable for nutrient management and modeling efforts. Here, estimated ammonium production from remineralization ranged from 103 to 180 $\mu\text{mol N m}^{-2} \text{h}^{-1}$ from 24 to 120 h in the $^{15}\text{NO}_3^-$ and $^{30}\text{N}_2$ treatments (Fig. 6). This rate is insufficient to balance the ammonium efflux measured in the OLW (328 \pm 24 to 345 \pm 46 $\mu\text{mol N m}^{-2} \text{h}^{-1}$ at 24 h and 276 to 429 $\mu\text{mol N m}^{-2} \text{h}^{-1}$ at 120 h). Ammonium production approaches the measured ammonium efflux when N-fixation rates from the $^{30}\text{N}_2$ cores (106 \pm 13 $\mu\text{mol N m}^{-2} \text{h}^{-1}$ at 24 h and 122 $\mu\text{mol N m}^{-2} \text{h}^{-1}$ at 120 h) are included.

N-fixation can also explain underestimated denitrification rates. Nitrate concentrations were very low (<0.2 μM) to undetectable in the OLW. When $\sim 5 \mu\text{M}$ nitrate was added to the inflowing water, nitrate concentrations in the outflow decreased over time (from $3.2 \pm 0.8 \mu\text{M}$ at 12 h to $0.61 \pm 0.05 \mu\text{M}$ at 120 h, Table 1). At 120 h, nitrate uptake flux was $-64 \mu\text{mol m}^{-2} \text{h}^{-1}$, but DNRA was not observed, and the highest measured potential denitrification rate was 40 $\mu\text{mol N m}^{-2} \text{h}^{-1}$. This result leaves approximately 24 μmol of N unaccounted for and may have underestimated the

denitrification rate. The potential denitrification rate is calculated based on the sum of the $^{28}\text{N}_2$, $^{29}\text{N}_2$, and $^{30}\text{N}_2$ fluxes and

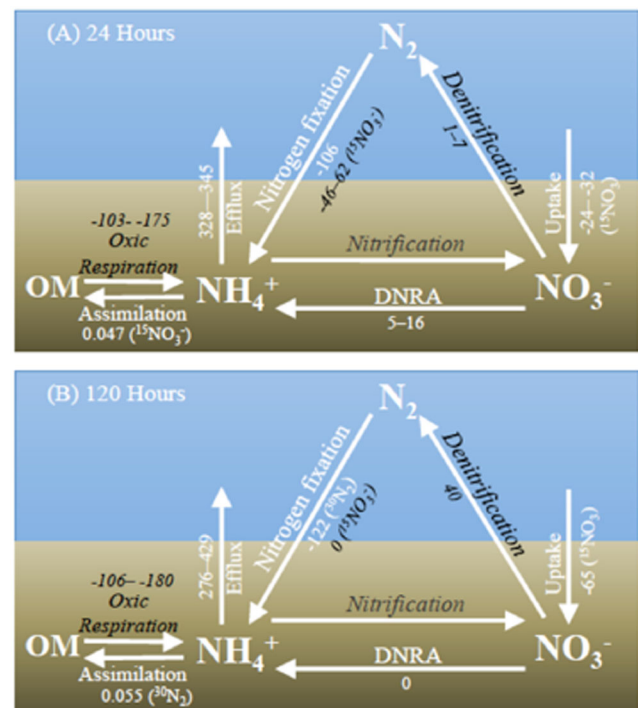


Fig. 6 N budget at the sediment-water interface at **a** 24 and **b** 120 h. Rates are reported in $\mu\text{mol N m}^{-2} \text{h}^{-1}$. Directly measured rates are shown in white: NH_4^+ and NO_3^- fluxes, N-fixation, DNRA, ^{15}N -assimilation to organic matter (OM), and calculated rates are shown in black: denitrification and N-fixation (An et al. 2001) and NH_4^+ remineralized from oxic respiration (calculated from SOD). Blue represents the OLW and brown the sediment. Nitrification (gray) was not measured, although significant rates are not required to balance the budget. ($^{30}\text{N}_2$) or ($^{15}\text{NO}_3^-$) following a rate indicates which core treatment the value was calculated/reported from

the calculated N-fixation rate, which may be underestimated by the same calculations, and cause an underestimate of denitrification. Thus, direct N-fixation estimates in sediment N budgets should be included to estimate a N mass balance accurately.

N inputs for a coastal N budget typically include river discharge, sewage, groundwater, urban runoff, atmospheric deposition, and pelagic N-fixation, while outputs include N loss via denitrification and anammox, or export to the ocean (Billen et al. 1985; Nixon et al. 1995). When sediment N-fixation is included, it usually refers to N-fixation in sediments in seagrass beds (Eyre and McKee 2002; Wulff et al. 2011), and those rates can be quite high, exceeding $410 \mu\text{mol N m}^{-2} \text{h}^{-1}$ (Eyre and McKee 2002). N-fixation in bare sediments is often excluded as an input, given the low rates measured indirectly (e.g., acetylene reduction) in the 1970s and 1980s (Howarth et al. 1988) or because it was not clearly required to balance the budget (Nixon et al. 1995). However, more recent rates reported in the literature and here suggest that sediment N-fixation may be on par with or a large percentage of N_2 loss pathways when averaged over time (Table 3). When the net N_2 flux varies between net N-fixation and denitrification, the ability of an estuary to mitigate excess nitrogen loading can vary greatly on an annual scale, making it critical to accurately measure the rates of both processes, as well as the N-loading. In Narragansett Bay, a nine year study showed that in some years, up to 25 % of the incoming N is removed through denitrification, while in other years, up to 30 % of the N is added through N-fixation (Fulweiler and Heiss 2014). The mean and maximum rates for N-fixation and potential denitrification measured in this paper (extrapolated to $\text{kg N ha}^{-1} \text{year}^{-1}$ over the 3.34 km^2 of Waquoit Bay) are the same order of magnitude as the total N load measured by Valiela et al. (2000) of $26,781 \pm 9.6 \text{ kg N year}^{-1}$ /N-fixation could be $48,000 \text{ kg N year}^{-1}$ (mean) to $75,000 \text{ kg N year}^{-1}$ (maximum) and denitrification could be $1500 \text{ kg N year}^{-1}$ (mean) to $16,000 \text{ kg N year}^{-1}$ (maximum). While the fluctuation in daily rates (from undetected to maximum rates) and the seasonal variability reported in Foster and Fulweiler (2014) suggested that the annual loss or load from denitrification and N-fixation are much lower than these maximum rates, these numbers emphasize both the potential contribution of N-fixation to an already eutrophic estuary, as well as the importance of the balance between these processes.

With a preponderance of evidence indicating dynamic sediment N_2 fluxes, constraining coastal marine N budgets may require a more thorough evaluation of N_2 flux pathways. Net sediment N_2 flux measurements throughout the year and over multiple years are critical to determining the balance of N_2 production and consumption. Quantifying production and

consumption individually may be necessary to model that balance over time. This study highlights the need to evaluate both N-fixation and denitrification, either using net N_2 fluxes or direct measurements of opposing pathways, to accurately model the coastal marine N budget.

Acknowledgments We thank Chris Weidman and the staff at WB-NERR for boat time and Sarah Foster, Hollie Emery, Kristin Yoshimura, and Kaitlyn Pritchard for assistance in the field and in the lab. We also thank Allen Hunt for his help with the diffusion calculations. SEN was funded by an NSF Postdoctoral Fellowship in Biology (1103692). This work was supported in part by funding from the Woods Hole Sea Grant to RWF, as well as the Sloan Foundation fellowship to RWF.

References

- An, S., and W.S. Gardner. 2002. Dissimilatory nitrate reduction to ammonium (DNRA) as a nitrogen link, versus denitrification as a sink in a shallow estuary (Laguna Madre/Baffin Bay, Texas). *Marine Ecology Progress Series* 237: 41–50.
- An, S., and S.B. Joye. 2001. Enhancement of coupled nitrification-denitrification by benthic photosynthesis in shallow estuarine sediments. *Limnology and Oceanography* 46(1): 62–74.
- An, S., W.S. Gardner, and T. Kana. 2001. Simultaneous measurement of denitrification and nitrogen fixation using isotope pairing with membrane inlet mass spectrometry analysis. *Applied and Environmental Microbiology* 67(3): 1171–1178.
- Bentzon-Tilia, M., S.J. Traving, M. Mantikci, H. Knudsen-Leerbeck, J.L. Hansen, S. Markager, and L. Riemann. 2015. Significant N_2 fixation by heterotrophs, photoheterotrophs and heterocystous cyanobacteria in two temperate estuaries. *The ISME Journal* 9(2): 273–285.
- Billen, G., M. Somville, E. De Becker, and P. Servais. 1985. A nitrogen budget of the Scheldt hydrographical basin. *Netherlands Journal of Sea Research* 19(3): 223–230.
- Boudreau, B.P. 1996. A method-of-lines code for carbon and nutrient diagenesis in aquatic sediments. *Computers & Geosciences* 22(5): 479–496.
- Bowen, J.L., and I. Valiela. 2001. The ecological effects of urbanization of coastal watersheds: Historical increases in nitrogen loads and eutrophication of Waquoit Bay estuaries. *Canadian Journal of Fisheries and Aquatic Sciences* 58(8): 1489–1500.
- Braker, G., A. Fesefeldt, and K.P. Witzel. 1998. Development of PCR primer systems for amplification of nitrite reductase genes (nirK and nirS) to detect denitrifying bacteria in environmental samples. *Applied and Environmental Microbiology* 64(10): 3769–3775.
- Brin, L.D., A.E. Giblin, and J.J. Rich. 2014. Environmental controls of anammox and denitrification in southern New England estuarine and shelf sediments. *Limnology and Oceanography* 59(3): 851–860.
- Brown, S.M., and B.D. Jenkins. 2014. Profiling gene expression to distinguish the likely active diazotrophs from a sea of genetic potential in marine sediments. *Environmental Microbiology* 16(10): 3128–3142.
- Brunet, R.C., and L.J. Garcia-Gil. 1996. Sulfide-induced dissimilatory nitrate reduction anaerobic freshwater sediments. *FEMS Microbiology Ecology* 21(2): 131–138.
- Burgin, A.J., and S.K. Hamilton. 2007. Have we overemphasized the role of denitrification in aquatic ecosystems? A review of nitrate removal pathways. *Frontiers in Ecology and the Environment* 5(2): 89–96.
- Capone, D.G., and E.J. Carpenter. 1982. Nitrogen fixation in the marine environment. *Science* 217(4565): 1140–1142.

- Capone, D.G., J.P. Zehr, H.W. Paerl, B. Bergman, and E.J. Carpenter. 1997. Trichodesmium, a globally significant marine cyanobacterium. *Science* 276(5316): 1221–1229.
- Cornwell, J.C., W.M. Kemp, and T.M. Kana. 1999. Denitrification in coastal ecosystems: Methods, environmental controls, and ecosystem level controls, a review. *Aquatic Ecology* 33(1): 41–54.
- Crank J. 1975. *The mathematics of diffusion*. 2nd Edition, Oxford University Press.
- Dalsgaard, T., B. Thamdrup, and D.E. Canfield. 2005. Anaerobic ammonium oxidation (anammox) in the marine environment. *Research in Microbiology* 156(4): 457–464.
- Desnoues, N., M. Lin, X. Guo, L. Ma, R. Carreño-Lopez, and C. Elmerich. 2003. Nitrogen fixation genetics and regulation in a *Pseudomonas stutzeri* strain associated with rice. *Microbiology* 149(8): 2251–2262.
- Eyre, B.D., and L.J. McKee. 2002. Carbon, nitrogen, and phosphorus budgets for a shallow subtropical coastal embayment (Moreton Bay, Australia). *Limnology and Oceanography* 47(4): 1043–1055.
- Eyre, B.D., S. Rysgaard, T. Dalsgaard, and P.B. Christensen. 2002. Comparison of isotope pairing and N₂:Ar methods for measuring sediment denitrification—assumption, modifications, and implications. *Estuaries* 25(6): 1077–1087.
- Eyre, B.D., D.T. Maher, and P. Squire. 2013. Quantity and quality of organic matter (detritus) drives N₂ effluxes (net denitrification) across seasons, benthic habitats, and estuaries. *Global Biogeochemical Cycles* 27.4(2013): 1083–1095.
- Fan Lu. 2013. Response of diazotrophic microbial community to nitrogen input and glyphosate application in soils cropped to soybean. Ph.D. Dissertation, Auburn University, Auburn.
- Ferguson, A., and B. Eyre. 2013. Interaction of benthic microalgae and macrofauna in the control of benthic metabolism, nutrient fluxes and denitrification in a shallow sub-tropical coastal embayment (western Moreton Bay, Australia). *Biogeochemistry* 112(1-3): 423–440.
- Foster, S.Q., and R.W. Fulweiler. 2014. Spatial and historic variability of benthic nitrogen cycling in an anthropogenically impacted estuary. *Frontiers in Marine Science* 1: 56.
- Foster, S. Q., and R.W. Fulweiler. (2015). Corrigendum: Spatial and historic variability of benthic nitrogen cycling in an anthropogenically impacted estuary. *Frontiers in Marine Science* 2: 70.
- Francis, C.A., K.J. Roberts, J.M. Beman, A.E. Santoro, and B.B. Oakley. 2005. Ubiquity and diversity of ammonia-oxidizing archaea in water columns and sediments of the ocean. *Proceedings of the National Academy of Sciences of the United States of America* 102(41): 14683–14688.
- Froelich, P., G.P. Klinkhammer, M.A.A. Bender, N.A. Luedtke, G.R. Heath, D. Cullen, et al. 1979. Early oxidation of organic matter in pelagic sediments of the eastern equatorial Atlantic: Suboxic diagenesis. *Geochimica et Cosmochimica Acta* 43(7): 1075–1090.
- Fulweiler, R.W., and E.M. Heiss. 2014. A decade of directly measured sediment N. *Oceanography* 27(1): 184.
- Fulweiler, R.W., S.W. Nixon, B.A. Buckley, and S.L. Granger. 2007. Reversal of the net dinitrogen gas flux in coastal marine sediments. *Nature* 448(7150): 180–182.
- Fulweiler, R.W., S.M. Brown, S.W. Nixon, and B.D. Jenkins. 2013. Evidence and a conceptual model for the cooccurrence of nitrogen fixation and denitrification in heterotrophic marine sediments. *Marine Ecology Progress Series* 482: 57–68.
- Fulweiler, R.W., Heiss, E. M., Rogener, M. K., Newell, S. E., LeClerc, G. R., Kortebein, S. M., & Wilhelm, S. W. 2015. Examining the impact of acetylene on N-fixation and the active sediment microbial community. *Frontiers in Microbiology* 6.
- Galloway, J.N., Leach, A.M., Bleeker, A., & Erisman, J.W. 2013. A chronology of human understanding of the nitrogen cycle. *Philosophical Transactions of the Royal Society B: Biological Sciences* 368(1621).
- Gardner, W. S., & McCarthy, M. J. 2006. Dissimilatory Nitrate Reduction to Ammonium (DNRA) as a “link” for N and a “sink” for oxygen in shallow, hypoxic, coastal environments. *EOS, Transactions, American Geophysical Union* 87(36).
- Gardner, W.S., and M.J. McCarthy. 2009. Nitrogen dynamics at the sediment–water interface in shallow, sub-tropical Florida Bay: Why denitrification efficiency may decrease with increased eutrophication. *Biogeochemistry* 95(2-3): 185–198.
- Gardner, W.S., and P.A. St. John. 1991. High-performance liquid chromatographic method to determine ammonium ion and primary amines in seawater. *Analytical Chemistry* 63(5): 537–540.
- Gardner, W.S., H.A. Bootsma, C. Evans, and P.A.S. John. 1995. Improved chromatographic analysis of ¹⁵N:¹⁴N ratios in ammonium or nitrate for isotope addition experiments. *Marine Chemistry* 48(3): 271–282.
- Gardner, W.S., M.J. McCarthy, S. An, D. Sobolev, K.S. Sell, and D. Brock. 2006. Nitrogen fixation and dissimilatory nitrate reduction to ammonium (DNRA) support nitrogen dynamics in Texas estuaries. *Limnology and Oceanography* 51(1): 558–568.
- Gardner, W.S., M.J. McCarthy, S.A. Carini, A.C. Souza, H. Lijun, K.S. McNeal, M.K. Puckett, and J. Pennington. 2009. Collection of intact sediment cores with overlying water to study nitrogen- and oxygen-dynamics in regions with seasonal hypoxia. *Continental Shelf Research* 29: 2207–2213.
- Giblin, A.E., C.R. Tobias, B. Song, N. Weston, G.T. Banta, and V.H. Rivera-Monroy. 2013. The importance of DNRA in the nitrogen cycle of coastal ecosystems. *Oceanography* 26: 124–131.
- Grantz, E.M., A. Kogo, and J. Thad Scott. 2012. Partitioning whole-lake denitrification using *in situ* dinitrogen gas accumulation and intact sediment core experiments. *Limnology and Oceanography* 57(4): 925–935.
- Grasshoff, K., Kremling, K., and Ehrhardt, M. (1999). *Methods of seawater analysis*. 3rd ed., eds.K. Grasshoff, K. Kremling, and M. Ehrhardt Wiley-VCH.
- Hamersley, R.M., and B.L. Howes. 2005. Evaluation of the N₂ flux approach for measuring sediment denitrification. *Estuarine Coastal and Shelf Science* 62(4): 711–723.
- Hartnett, H.E., and S.P. Seitzinger. 2003. High-resolution nitrogen gas profiles in sediment porewaters using a new membrane probe for membrane-inlet mass spectrometry. *Marine Chemistry* 83(1): 23–30.
- Heiss, E.M., L. Fields, and R.W. Fulweiler. 2012. Directly measured net denitrification rates in offshore New England sediments. *Continental Shelf Research* 45: 78–86.
- Hopkinson, C.S., I. Buffam, J. Hobbie, J. Vallino, M. Perdue, B. Eversmeyer, et al. 1998. Terrestrial inputs of organic matter to coastal ecosystems: An intercomparison of chemical characteristics and bioavailability. *Biogeochemistry* 43(3): 211–234.
- Howarth, R. W., Marino, R., & Cole, J. J. 1988. Nitrogen fixation in freshwater, estuarine, and marine ecosystems. 2. Biogeochemical controls. *Limnology and Oceanography* 688–701.
- Kana, T.M., and D.L. Weiss. 2004. Comment on “Comparison of isotope pairing and N₂:Ar methods for measuring sediment denitrification” by BD Eyre, S. Rysgaard, T. Dalsgaard, and P. Bondo Christensen. *Estuaries and Coasts* 27(1): 173–176.
- Kana, T.M., C. Darkangelo, M.D. Hunt, J.B. Oldham, G.E. Bennett, and J.C. Cornwell. 1994. Membrane inlet mass spectrometer for rapid high-precision determination of N₂, O₂, and Ar in environmental water samples. *Analytical Chemistry* 66(23): 4166–4170.
- Kartal, B., M.M. Kuypers, G. Lavik, J. Schalk, H.J. Op den Camp, M.S. Jetten, and M. Strous. 2007. Anammox bacteria disguised as denitrifiers: Nitrate reduction to dinitrogen gas via nitrite & ammonium. *Environmental Microbiology* 9(3): 635–642.
- Knapp, A. N. 2012. The sensitivity of marine N₂ fixation to dissolved inorganic nitrogen. *Frontiers in microbiology* 3.

- Koike, I., and A. Hattori. 1978. Simultaneous determinations of nitrification and nitrate reduction in coastal sediments by a ^{15}N dilution technique. *Marine Ecology-Progress Series* 35: 853–857.
- Koop-Jakobsen, K., and A.E. Giblin. 2010. The effect of increased nitrate loading on nitrate reduction via denitrification and DNRA in salt marsh sediments. *Limnology and Oceanography* 55(2): 789.
- Körner, H., and W.G. Zumft. 1989. Expression of denitrification enzymes in response to the dissolved oxygen level and respiratory substrate in continuous culture of *Pseudomonas stutzeri*. *Applied and Environmental Microbiology* 55(7): 1670–1676.
- Lam, P., Lavik, G., Jensen, M. M., van de Vossenberg, J., Schmid, M., Woebken, D.,... & Kuypers, M. M. 2009. Revising the nitrogen cycle in the Peruvian oxygen minimum zone. *Proceedings of the National Academy of Sciences* 106(12):4752–4757.
- LaMontagne, M.G., V. Astorga, A.E. Giblin, and I. Valiela. 2002. Denitrification and the stoichiometry of nutrient regeneration in Waquoit Bay, Massachusetts. *Estuaries* 25(2): 272–281.
- Lindell, D., and A.F. Post. 2001. Ecological aspects of ntcA gene expression and its use as an indicator of the nitrogen status of *Marine Synechococcus* spp. *Applied and Environmental Microbiology* 67(8): 3340–3349.
- McCarthy, M.J., S.A. Carini, Z. Liu, N.E. Ostrom, and W.S. Gardner. 2013. Oxygen consumption in the water column and sediments of the northern Gulf of Mexico hypoxic zone. *Estuarine Coastal and Shelf Science* 123: 46–53.
- McCarthy, M. J., Newell, S. E., Carini, S. A., & Gardner, W. S. 2015. Denitrification dominates sediment nitrogen removal and is enhanced by bottom-water hypoxia in the Northern Gulf of Mexico. *Estuaries and Coasts* 1–16.
- Mortazavi, B., A.A. Riggs, J.M. Caffrey, H. Genet, and S.W. Phipps. 2012. The contribution of benthic nutrient regeneration to primary production in a shallow eutrophic estuary, Weeks Bay, Alabama. *Estuaries and Coasts* 35(3): 862–877.
- Mulder, A., A.A. Van de Graaf, L.A. Robertson, and J.G. Kuenen. 1995. Anaerobic ammonium oxidation discovered in a denitrifying fluidized-bed reactor. *FEMS Microbiology Ecology* 16(3): 177–183.
- Newell, S. E., Babbin, A. R., Jayakumar, A., & Ward, B. B. 2011. Ammonia oxidation rates and nitrification in the Arabian Sea. *Global Biogeochemical Cycles* 25(4)
- Nixon, S.W., S.L. Granger, and B.L. Nowicki. 1995. An assessment of the annual mass balance of carbon, nitrogen, and phosphorus in Narragansett Bay. *Biogeochemistry* 31(1): 15–61.
- Owens, N.J.P. 1988. Rapid and total automation of shipboard ^{15}N analysis: Examples from the North Sea. *Journal of Experimental Marine Biology and Ecology* 122(2): 163–171.
- Poly, F., L.J. Monrozier, and R. Bally. 2001. Improvement in the RFLP procedure for studying the diversity of nifH genes in communities of nitrogen fixers in soil. *Research in Microbiology* 152(1): 95–103.
- Scott, J.T., M.J. McCarthy, W.S. Gardner, and R.D. Doyle. 2008. Denitrification, dissimilatory nitrate reduction to ammonium, and nitrogen fixation along a nitrate concentration gradient in a created freshwater wetland. *Biogeochem* 87(1): 99–111.
- Seitzinger, S.P., and J.H. Garber. 1987. Nitrogen fixation and $^{15}\text{N}_2$ calibration of the acetylene reduction assay in coastal marine sediment. *Marine Ecology Progress Series* 37: 65–73.
- Seitzinger, S.P., W.S. Gardner, and A.K. Spratt. 1991. The effect of salinity on ammonium sorption in aquatic sediments: Implications for benthic nutrient recycling. *Estuaries* 14(2): 167–174.
- Solorzano, L. 1969. Determination of ammonia in natural waters by the phenylhypochlorite method. *Limnology and Oceanography* 14: 799–801.
- Tiedje, J.M. 1988. Ecology of denitrification and dissimilatory nitrate reduction to ammonium. *Biology of Anaerobic Microorganisms* 717: 179–244.
- Valiela, I., M. Geist, J. McClelland, and G. Tomasky. 2000. Nitrogen loading from watersheds to estuaries: Verification of the Waquoit Bay nitrogen loading model. *Biogeochemistry* 49(3): 277–293.33.
- Vieillard, A.M., and R.W. Fulweiler. 2012. Impacts of long-term fertilization on salt marsh tidal creek benthic nutrient and N_2 gas fluxes. *Marine Ecology Progress Series* 471: 11–22.
- Ward, B. B., Devol, A. H., Rich, J. J., Chang, B. X., Bulow, S. E., Naik, H.,... & Jayakumar, A. 2009. Denitrification as the dominant nitrogen loss process in the Arabian Sea. *Nature* 461(7260):78–81.
- Welsh, D.T. 2000. Nitrogen fixation in seagrass meadows: Regulation, plant–bacteria interactions and significance to primary productivity. *Ecology Letters* 3(1): 58–71.
- Wulff, F., B.D. Eyre, and R. Johnstone. 2011. Nitrogen versus phosphorus limitation in a subtropical coastal embayment (Moreton Bay; Australia): Implications for management. *Ecological Modelling* 222(1): 120–130.
- Zehr, J.P., and P.J. Turner. 2001. 14 nitrogen fixation: Nitrogenase genes and gene expression. *Marine Microbiology* 30: 271.